Cell Biol Toxicol (2022) 38:167–183
https://doi.org/10.1007/s10565-021-09585-1

ORIGINAL ARTICLE

The aberrant cross-talk of epithelium–macrophages via METTL3-regulated extracellular vesicle miR-93 in smoking-induced emphysema

Haibo Xia · Yan Wu · Jing Zhao · Wenqi Li · Lu Lu · Huimin Ma · Cheng Cheng · Jing Sun · Quanyong Xiang · Tao Bian · Qizhan Liu

Received: 26 November 2020 / Accepted: 1 February 2021 / Published online: 4 March 2021

Abstract Cigarette smoke (CS), a complex chemical indoor air pollutant, induces degradation of elastin, resulting in emphysema. Aberrant cross-talk between macrophages and bronchial epithelial cells is essential for the degradation of elastin that contributes to emphysema, in which extracellular vesicles (EVs) play a critical role. The formation of N6-methyladenosine (m6A) is a modification in miRNA processing, but its role in the development of emphysema remains unclear. Here, we established that production of excess mature microRNA-93 (miR-93) in bronchial epithelial cells via enhanced m6A modification was mediated by overexpressed methyltransferase-like 3 (METTL3) induced by CS. Mature miR-93 was transferred from

Haibo Xia, Yan Wu and Jing Zhao contributed equally to this work.

Highlights 1. CSE increases levels of METTL3 and miR-93 with a dose-dependent manner in HBE cells.
2. CSE promotes miR-93 maturation via METTL3-mediated m6A modification in HBE cells.
3. CS induces the degradation of elastin in lung tissue due to elevation of MMP9 and MMP12 in macrophages.
4. EV miR-93 mediates the aberrant cross-talk of epithelium–macrophages in CS-induced emphysema.

H. Xia · J. Zhao · W. Li · L. Lu · H. Ma · C. Cheng · J. Sun · Q. Liu
Center for Global Health, The Key Laboratory of Modern Toxicology, Ministry of Education, School of Public Health, Nanjing Medical University, Nanjing 211166 Jiangsu, People's Republic of China

H. Xia · J. Zhao · W. Li · L. Lu · H. Ma · C. Cheng · J. Sun · Q. Liu (✉)
China International Cooperation Center for Environment and Human Health, Jiangsu Key Laboratory of Cancer Biomarkers, Prevention and Treatment, Jiangsu Collaborative Innovation Center for Cancer Personalized Medicine, School of Public Health, Nanjing Medical University, Nanjing 211166 Jiangsu, People's Republic of China
e-mail: drqzliu@hotmail.com

Y. Wu · T. Bian (✉)
Department of Respiratory and Critical Care Medicine, Wuxi People's Hospital Affiliated to Nanjing Medical University, Wuxi 214023 Jiangsu, People's Republic of China
e-mail: biantaophd@126.com

Q. Xiang
Jiangsu Provincial Center for Disease Control and Prevention, Nanjing 210009 Jiangsu, People's Republic of China

bronchial epithelial cells into macrophages by EVs. In macrophages, miR-93 activated the JNK pathway by targeting dual-specificity phosphatase 2 (DUSP2), which elevated the levels of matrix metalloproteinase 9 (MMP9) and matrix metalloproteinase 12 (MMP12) and induced elastin degradation, leading to emphysema. These results demonstrate that METTL3-mediated formation of EV miR-93, facilitated by m6A, is implicated in the aberrant cross-talk of epithelium–macrophages, indicating that this process is involved in the smoking-related emphysema. EV miR-93 may use as a novel risk biomarker for CS-induced emphysema.

Keywords Emphysema · Cigarette smoke · N6-methyladenosine · Extracellular vesicles · MicroRNAs

Introduction

Cigarette smoke (CS), an indoor air pollutant, has strong oxidizing, pro-inflammatory, and carcinogenic properties (Miao et al. 2019). In developed countries, smoking is the main risk factor for COPD (Seimetz et al. 2011). For lung tissues, CS increases the recruitment of leukocytes, which release mediators of inflammation, proteinases that promote inflammation and injury (De Smet et al. 2019). The extracellular matrix (ECM) of alveoli serves as a scaffold supporting the respiratory function. Permanent airspace enlargement occurs through the destruction of alveolar wall matrix structures, which is accomplished by macrophage production of matrix metalloproteinases (MMPs) (Jeon et al. 2019). Thus, MMPs participate in destruction of the alveolar extracellular matrix and promote the pathogenesis of emphysema. The mechanism involved warrants further investigation.

Macrophage-derived MMPs promote emphysema (Selman et al. 2003). MMPs, proteolytic enzymes, play roles in ECM remodeling, cell migration, and tissue defense; however, excess MMPs leads to tissue destruction (Brinckerhoff and Matrisian 2002). Several MMPs are elevated in emphysema. In particular, MMP-9 and MMP-12 are relevant to development of emphysema (Elkington and Friedland 2006; Gueders et al. 2006). MMP-9 degrades elastin and is implicated in the lung destruction that is characteristic of COPD (Sng et al. 2017). MMP12 is responsible for degradation of basement membrane structures by macrophages (Shipley et al. 1996). As much as 50% of the elastolytic activity in bronchoalveolar lavage fluid (BALF) from smokers is attributable to MMPs (Janoff et al. 1983).

Extracellular vesicles (EVs) are secreted by various cells, including epithelial cells and dendritic cells (Wahlgren et al. 2012). Aberrant cross-talk of epithelium–macrophages play an critical role in the pathogenesis of emphysema (He et al. 2019). EVs exert their effects by delivering their cargo, nucleic acids and protein, to various cells (O'Farrell and Yang 2019). As a cargo in EVs, microRNAs (miRNAs) participate in the pathogenesis of inflammatory lung diseases (Oglesby et al. 2010). Thus, miRNAs transported by EVs could influence the development of such diseases.

CS causes the aberrant expression of miRNAs, and such expression could lead to emphysema (Dang et al. 2017). METTL3, the main enzyme for production of N6-methyladenosine (m6A), perturbs miRNA maturation via modifying primary miRNAs; this process participates in various pathophysiological processes (Cheng et al. 2019). CS condensate induces hypomethylation of *CpG* island in the METTL3, resulting in abnormal elevation of METTL3 (Zhang et al. 2019). METTL3 promotes the maturation of miR-93 by interacting with the microprocessor protein, DGCR8, via the m6A modification on primary- (pri-)miRNAs (Alarcon et al. 2015). Although miR-93 is involved in various respiratory diseases (Yang et al. 2018), its role in the pathogenesis of emphysema is undefined.

Here, we report that the upregulation of EV miR-93 in bronchial epithelium exposed to CS disturbs the cross-talk between these cells and macrophages and elevates the expression of MMPs by macrophages. Specifically, CS induces METTL3 increasing, which elevates m6A modification in pri-miR-93 and promotes the maturation of miR-93. EVs carry excess miR-93 from bronchial epithelial cells to macrophages, which target and suppress the expression of dual-specificity phosphatase 2 (DUSP2) mRNA. In macrophages, reduced DUSP2 expression induces JNK/c-Jun signaling and promotes the expression of MMPs, destruction of alveolar wall matrix structures, and the initiation and progression of emphysema.

Methods

Patients and Samples

This study was approved by the Ethics Committee of Wuxi People's Hospital. Each patient participating in the

study signed (and/or their families signed) a written informed consent. According to the GOLD guidelines (Vogelmeier et al. 2017), COPD patients were defined as those who had dyspnea and a history of exposure to risk factors for the disease along with a FEV1/FVC ratio of < 70% as determined at Wuxi People's Hospital. In addition, normal lung tissues were acquired during resection surgeries for benign lung nodules. Based on the smoking history and diagnosis, samples were divided into a non-smoker group, a smoker group, and a COPD smoker group. Characteristics of subjects are presented in Table 1.

In vivo and in vitro experiments

Supplementary methods

Statistical analyses

All experiments were performed in triplicate. Derived values are presented as means ± SEM or means ± SD. Comparison of means between two groups was conducted by using Student's *t* test. Data in abnormal distribution were analyzed by nonparametric test. Spearman's correlations were calculated between miR-93 levels and FEV_1/FVC (%) of COPD patients. Correlations were considered significant and positive when $P < 0.05$ and $R^2 > 0.30$. All statistical analyses were performed with SPSS 17.0. *P* values < 0.05 were considered statistically significant.

Results

CS induces inflammation, increases of METTL3, miR-93, and MMPs, and emphysema in lung tissues of mice

To identify factors regulating emphysema, comparisons were made for mice exposed either to air or to various concentrations (100, 200, or 300 mg/m^3 TPM) of CS for 0, 8, or 16 weeks. The various concentrations of CS caused different degrees of emphysema, in which there were dose–effect and time–effect relationships, including irregular enlargement of airspaces throughout the parenchyma (Fig. 1a, b). For mice exposed to the high concentrations of CS, there were higher numbers of total cells, monocytes, and neutrophils in the BALF (Fig. 1c, e), indicating that CS induces inflammation in their lungs.

METTL3 perturbs miRNA maturation via modifying primary miRNAs (Cheng et al. 2019). Since METTL3 is involved in miRNA processing, we selected five miRNAs (miR-335, miR-93, miR-221, miR-222, and miR-25) with the most significant changes upon METTL3 downregulation and overexpression (Alarcon et al. 2015). METTL3 promotes the maturation of miR-93 by interacting with the microprocessor protein, DGCR8, via the m6A modification on primary-(pri-)miRNAs (Alarcon et al. 2015). To elucidate the effects CS on RNA m6A levels and its mechanisms, we analyzed, in lung tissues of mice, the RNA m6A levels in total RNA and the mRNA levels of m6A modification-related enzymes (Mettl3, Mettl14, Wtap, Fto, and Alkbh5). CS induced increases of Mettl3, Mettl14, and Alkbh5 mRNA and decreases of levels of Fto mRNA (Table 2). The mRNA levels of Mettl3 were increased, with a CS concentration-dependent manner (Fig. S1).

In determining the effects of CS on miR-335, miR-93, miR-221, miR-222, and miR-25 in lung tissues of mice, we found that the most significantly increased miRNA was miR-93, with a CS concentration dependence; the other four miRNAs had no appreciable changes (Figs. S2 and 1f). With higher CS concentrations, the levels of METTL3, p-JNK, p-c-Jun, MMP9, and MMP12 were elevated, but the levels of DUSP2 and elastin were low in lung tissues of mice (Fig. 1g, h). These results reveal that, for mice, CS induces lung inflammation; increased levels of METTL3, miR-93, and MMPs; and emphysema.

CSE promotes miR-93 maturation via METTL3-mediated m6A modification

CS causes hypomethylation of METTL3, which induces its overexpression (Zhang et al. 2019). METTL3-mediated m6A modifications label pri-miRNAs and recognize DGCR8 molecules, promoting maturation of miRNAs and leading to their differential expression in various biological processes (Wang et al. 2019). Thus, METTL3 was overexpressed in lung tissues of mice with emphysema induced by CS exposure (Fig. 1g, h). Therefore, METTL3 levels and the levels of pri-miR-93, pre-miR-93, and miR-93 were measured to identify which was responsible for the CSE-induced damage to HBE cells. HBE cells were exposed to different concentrations of CSE for 48 h. With increasing CSE concentrations, there were elevated METLL3 levels as

determined by Western blot and immunofluorescence assays (Fig. 2a–c). Also, with increasing concentrations of CSE, pri-miR-93 levels decreased, but pre-miR-93 and miR-93 levels increased (Fig. 2d).

METTL3-mediated m6A is a post-transcriptional modification that promotes miRNA biogenesis (Alarcon et al. 2015). To revel the mechanism of CSE induces METTL3-induced miR-93 maturation, a METTL3 siRNA was transfected into CSE-treated HBE cells (CHBE cells), which lowered the levels of METTL3 (Fig. 2e, f). Moreover, compared with CHBE cells, these cells transfected with METTL3 siRNA showed relatively high levels of pri-miR-93, but with low levels of pre-miR-93 and miR-93 (Fig. 2g). Next, we identified the m6A modification site on pri-miR-93 by SRAMP (Fig. 2h). RNA immunoprecipitation (RIP) with METTL3 and m6A antibodies followed by qRT-PCR revealed recruitment of pri-miR-93 in HBE cells; however, cells transfected with METTL3 siRNA showed relatively low levels of pri-miR-93 in immunoprecipitated RNA (Fig. 2i, k). Moreover, compared with CHBE cells, these cells transfected with METTL3 siRNA showed relatively low levels of m6A in total RNA (Fig. 2j). These results demonstrate that, for HBE cells, the higher miR-93 levels caused by CS exposure could be the consequence of promoted maturation of miR-3 via m6A modification by increased, CS-induced METTL3.

Decreases of METTL3 in CHBE cells blocks the increased miR-93 and MMPs levels in THP-M cells co-cultured with CHBE cells

To determine whether METTL3-induced miR-93 maturation via the m6A modification plays a critical role in the dysfunctional cross-talk of the bronchial epithelial and THP-M, macrophage-like cells, differentiated from THP-1 monocytes, were co-cultured for 48 h with control HBE cells or CHBE cells (Fig. 3a). miR-93 levels were high in THP-M cells co-cultured with CHBE cells, but not in THP-M cells co-cultured with HBE cells (Fig. 3b). Also, the levels of MMP9 and MMP12 were higher in THP-M cells co-cultured with CHBE cells than in those co-cultured with HBE cells (Fig. 3c, d). Moreover, we explored, with HBE cells, the effects of METTL3-induced miR-93 maturation via m6A modification on expression of MMPs by THP-M cells. The low levels of miR-93 in THP-M cells co-cultured with CHBE cells transfected with METTL3 siRNA (Fig. 3e). In THP-M cells co-cultured with METTL3 downregulated CHBE cells, the levels of MMP9 and MMP12 expression were lower (Fig. 3f, g). These results demonstrate that METTL3-mediated miR-93 derived from CHBE cells regulates the expression of MMPs by THP-M cells.

EVs derived from CHBE cells transfer miR-93 to THP-M cells to promote the expression of MMPs

EVs, as carriers of miRNAs, participate in the pathogenesis of inflammatory pulmonary diseases (Oglesby et al. 2010). Therefore, we hypothesized that EVs, from HBE cells, deliver miR-93 into THP-M cells. EVs from HBE and CHBE cells, named as HBE-EV and CHBE-EV, were isolated, characterized, and quantified. The surface markers (CD9, CD63, and CD81) of HBE-EV or CHBE-EV were evident; HSP90B1, a marker for endoplasmic reticulum, was minimal expression in these preparations (Fig. 4a). Moreover, TEM showed that the diameters of HBE-EV and CHBE-EV are less than 200

Table 1 Characteristics of subjects

	Non-smokers	Smokers	COPD smokers
Number	26	25	26
Males, *n* (%)	19 (73.1%)	25 (100%)	26 (100%)
Age, years	56 ± 7	55 ± 12	67.7±7.3*#
Smoking history, pack-years	0	22.4 ± 17.5	37.9 ± 22#
FEV_1/FVC (%)			54.83 + 10.63

Data are presented as means ± SD, unless otherwise stated

*$P < 0.01$ versus normal group, # $P < 0.01$ versus smoker group

nm; these EVs had cup- or sphere-shaped morphology (Fig. 4b). NTA analysis proved that particle sizes and counts with no significant differences between HBE-EV and CHBE-EV (Fig. 4c). HBE-EV or CHBE-EV treated with PKH67, a green fluorescent linker for membrane labeling, was added to THP-M cells. After 3 h, THP-M cells exhibited green fluorescent, indicating they had internalized the EVs (Fig. 4d). miR-93 levels were elevated in CHBE-EV (Fig. 4e) and were higher in THP-M cells treated with CHBE-EV than in those treated with HBE-EV (Fig. 4f). There were greater elevations of MMP9 and MMP12 in these cells exposed to CHBE-EV than in those exposed to HBE-EV (Fig. 4g, h). To assess the contributions of MMPs to elastin

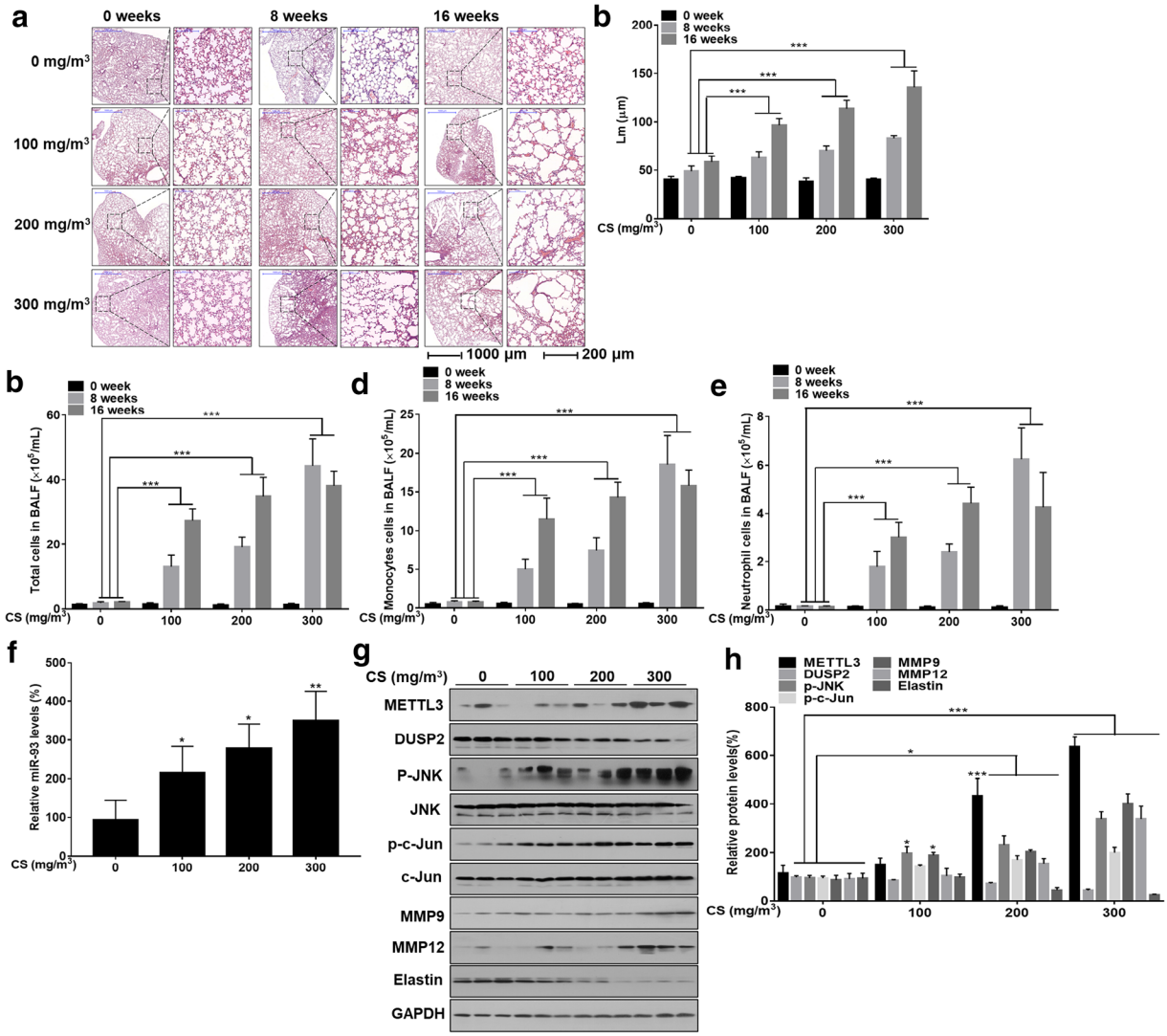

Fig. 1 CS induces emphysema, inflammation, increases of METTL3 and miR-93 levels, and activation of DUSP2/JNK/c-Jun in lung tissues of mice. Densities of bands were quantified by the ImageJ software. GAPDH levels, measured in parallel, served as controls. Male BALB/c mice at 6–8 weeks of age were exposed to 0, 100, 200, or 300 mg/m^3 TPM CS for 0, 8, or 16 weeks. **a** Representative images of lung sections after H&E staining (bars: left = 1000 μm, right = 200 μm) and **b** mean chord length (Lm) in lung tissues of mice. Counts of total cells (**c**), mononuclear cells (**d**), and neutrophils (**e**) in the BALF of mice. Male BALB/c mice at 6–8 weeks of age were exposed to 0, 100, 200, or 300 mg/m^3 TPM CS for 16 weeks. **f** The levels of miR-93 in lung tissues of mice were determined by qRT-PCR. **g** Western blots were performed, and **h** relative protein levels of METTL3, DUSP2, p-JNK, p-c-Jun, MMP9, MMP12, and elastin in lung tissues of mice were determined. All bars are presented as means ± SEM ($n = 6$). *$P <$ 0.05, **$P < 0.01$, and ***$P < 0.001$, different from the 0 mg/m^3 CS group

degradation, activity against an FITC-tagged elastin substrate was assessed. Elastin is a substrate for MMPs. THP-M cells exposed to CHBE-EV showed greater elastin degradation (Fig. 4i). These results indicate that EVs derived from CHBE cells transfer miR-93 to THP-M cells, which elevates expression of MMPs in these cells.

EV miR-93 derived from CHBE cells promotes the expression of MMPs by THP-M cells

To confirm that EV miR-93, derived from CHBE cells and transferred into THP-M cells, is involved in the expression of MMPs by THP-M cells, THP-M cells were co-culture with CHBE cells pretreated with GW4869, an inhibitor of EV biogenesis (Xu et al. 2018). The counts of EVs, released from CHBE cells, were decreased by GW4869 (Fig. 5a). The increased levels of miR-93 in THP-M cells co-cultured with CHBE cells were blocked by GW4869 (Fig. 5b). Further, the elevated levels of MMP9 and MMP12 in THP-M cells co-cultured with CHBE cells were attenuated by GW4869 (Fig. 5c, d). Knocking down miR-93 reduced the miR-93 levels in EVs of CHBE cells (Fig. 5e), which induced lower levels of miR-93 in THP-M cells (Fig. 5f). In addition, downregulation of EV miR-93 blocked the EV-induced MMP9 and MMP12 elevations in THP-M cells (Fig. 5g, h). Compared to exposure to EVs released from CHBE cells, THP-M cells treated with EVs released from miR-93 knockdown CHBE cells showed lower activity of elastin degradation (Fig. 5i). Thus, these experiments demonstrate that miR-93 is transferred from CHBE cells into THP-M cells via EVs and that it is involved in degrading elastin in a manner that is largely dependent on MMPs.

EV miR-93 regulates JNK pathway activation by DUSP2, which is involved in expression of MMPs in THP-M cells

Activation of the JNK pathway is a factor in the promotion of MMP overexpression by macrophages (Lv et al. 2019; Wu et al. 2001). To prove whether the JNK pathway regulates the expression of MMPs in macrophages, Western blots were performed. The protein levels of p-JNK and p-c-Jun were upregulated in THP-M cells treated with EVs released from CHBE cells (Fig. 6a, b). By using online databases miRmap (mirmap.ezlab.org), Targetscan (targetscan.org), and Miranda (microrna.org), we predicted the targets of miR-93, DUSP2, a factor contributed to JNK dephosphorylation (Jeffrey et al. 2006). Meanwhile, DUSP2 levels were decreased in THP-M cells treated with CHBE-EV (Fig. 6a–c).

We thus performed the predicted binding site of miR-93 on DUSP2 3′-UTR sequences (Fig. 6d). There was lower luciferase activity for the vector containing wild-type DUSP2 3′-UTR, relative to that for the mutant

Table 2 Primer sequences used

pri-miR-93	F: 5′-*GGGGTCTGTTTCACTCCATGT*-3′ R: 5′-*CACGAACAGCACTTTGGAGC*-3′
pre-miR-93	F: 5′-*CTCCAAAGTGCTGTTCGTGC*-3′
	R: 5′-*GGGGCTCGGGAAGTGCTA*-3′
miR-93-RT	5′-*GTCGTATCCAGTGCGTGTCGTGGAGTCGGCAATTGC ACTGGATACGACCTACCT*-3′
U6-RT	5′-*AAAATATGGAACGCTTCACG*-3′
miR-93	F: 5′-*GGGGATGGACGTGCTTGTCG*-3′
	R: 5′-*CAGTGCGTGTCGTGGAGT*-3′
U6	F: 5′-*CGCTTTCGGCAGCACATATACTAAAATTGGAAC*-3′
	R: 5′-*GCTTCACGAATTTGCGTGTCATCCTTGC*-3′
GAPDH	F: 5′-*GGAGCGAGATCCCTCCAAAAT*-3′
	R: 5′-*GGCTGTTGTCATACTTCTCATGG*-3′
mmu-Gapdh	F: 5′-*GTCTTCACTACCATGGAGAAGG*-3′
	R: 5′-*TCATGGATGACCTTGGCCAG*-3′

DUSP2 3′-UTR, in the overexpression of miR-93 (induced by an miR-93 mimic) in THP-M cells (Fig. 6e). Moreover, CHBE-EV repressed the luciferase activity of the DUSP2 3′-UTR, compared to mutant DUSP2 3′-UTR (Fig. 6f). Additional experiments showed that DUSP2 levels were low in THP-M cells with miR-93 elevation but high with miR-93 downregulation (Fig. 6g, h). Further, inhibition of miR-93 prevented the elevation of p-JNK, p-c-Jun, and MMP9 and MMP12 levels caused by CHBE-EV (Fig. 6g, h). These results show that the miR-93-DUSP2-JNK regulatory axis is present in THP-M cells and that it participates in expression of MMPs by these cells.

METTL3-mediated EV miR-93, via DUSP2, is involved in c-Jun/JNK activation and expression of MMPs by THP-M cells

Consistent with Western blots results (Fig. 7a, b), knockdown of METTL3 alleviated the decrease of DUSP2 levels induced by CHBE-EV (Fig. 7c). Further, knocking down METTL3 in HBE cells blocked activation of the JNK pathway and the elevates of MMP9 and MMP12 levels that were caused by EVs derived from CHBE cells (Fig. 7a, b). Compared with THP-M cells treated with CHBE-EV, cultures of these cells treated with EVs derived from METTL3-

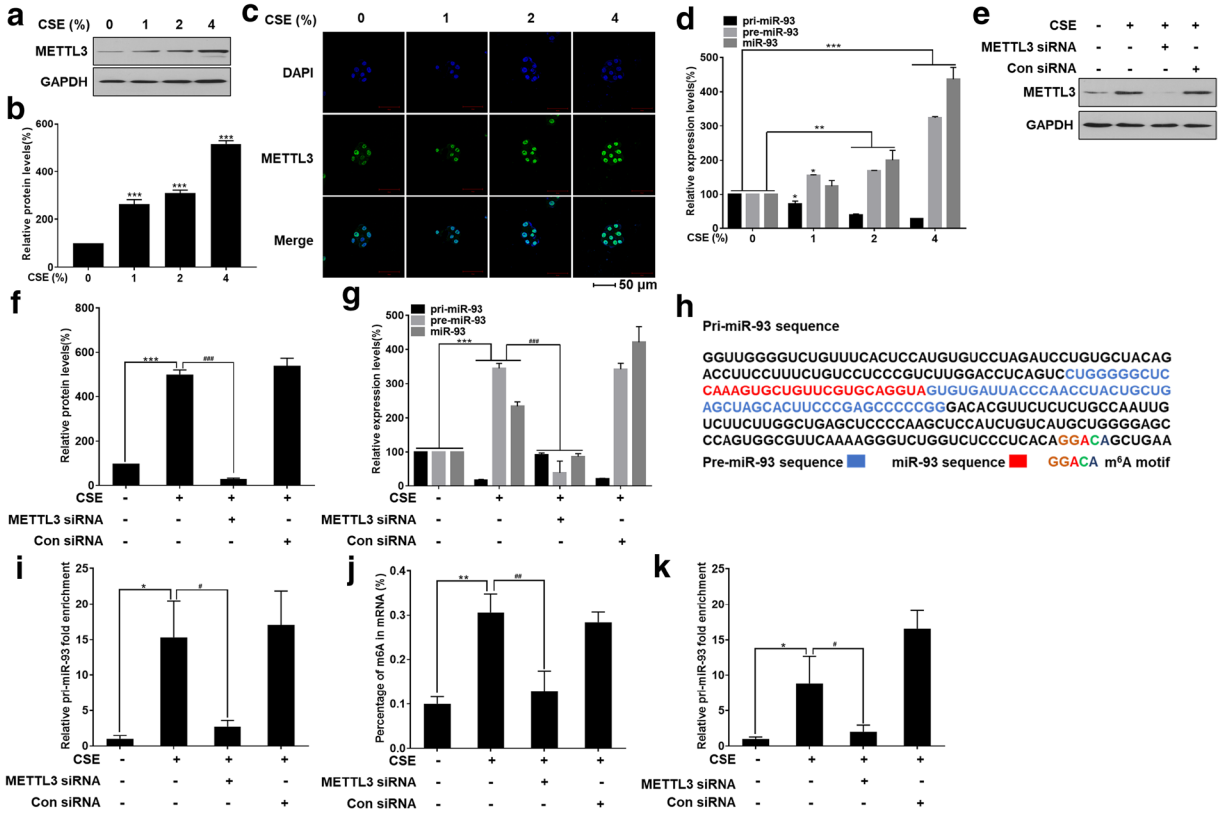

Fig. 2 CSE promotes miR-93 maturation via METTL3-mediated m6A modification in HBE cells. Densities of bands were quantified by the ImageJ software. GAPDH levels, measured in parallel, served as controls. HBE cells were treated with 0, 1, 2, or 4% CSE for 48 h. **a** Western blots were performed, and **b** relative protein levels of METTL3 were determined. **c** Immunofluorescence staining of METTL3 (green) and nuclei (blue) (bar: 50 μm). **d** The levels of pri-miR-93, pre-miR-93, and miR-93 determined by qRT-PCR. After HBE cells were transfected with 20 nM METTL3 siRNA or con siRNA, cells were treated with 0 or 4% CSE for 48 h. **e** Western blots were performed, and (**f**) relative protein levels of METTL3 were determined. **g** The levels of pri-miR-93, pre-miR-93, and miR-93 were determined by qRT-PCR. **h** The sequences of pri-miR-93, pre-miR-93, and miR-93 are highlighted by different colors; the m6A motif (GGACA) is located at the putative splicing site. **i** The levels of pri-miR-93 binding to METTL3 as determined by qRT-PCR after METTL3 Ab-treated RIP assays. **j** The levels of overall m6A in mRNA measured colorimetrically. **k** The levels of pri-miR-93 binding to m6A, measured by qRT-PCR, after m6A Ab-treated RIP assays. All bars are presented as means ± SD ($n = 3$). $^{*}P < 0.05$, $^{**}P < 0.01$, and $^{***}P < 0.001$, different from non-treated HBE cells, $^{\#}P < 0.05$, $^{\#\#}P < 0.01$, and $^{\#\#\#}P < 0.001$, different from CHBE cells

knockdown CHBE cells showed less activity of elastin degradation (Fig. 7d).

To determine if EV miR-93 derived from CHBE cells mediates expression of MMPs through regulation of DUSP2 in THP-M cells, control or DUSP2 siRNA-transduced THP-M cells were treated with CHBE-EV cells with or without transfection of an miR-93 inhibitor, and the levels of DUSP2, p-JNK, p-c-Jun, MMP9, and MMP12 were determined. Furthermore, ChIP assays proved that c-Jun bound to the promoter of the MMP9 and MMP12 gene after THP-M cells were treated with CHBE-EV (Fig. 7e). As shown by Western blotting, inhibition of miR-93 blocked the changes of DUSP2, p-JNK, p-c-Jun, MMP9, and MMP12 expression in THP-M cells caused by CHBE-EV, but downregulation of DUSP2 reversed the effects of the miR-93 inhibitor (Fig. 7f, g). Moreover, fluorescent elastin degradation assays proved that inhibition of miR-93 blocked the changes in elastin degradation of THP-M cells caused by CHBE-EV, but downregulation of DUSP2 reduced the effects of the miR-93 inhibitor (Fig. 7h). These results show that METTL3-mediated EV miR-93, via DUSP2, is involved in c-Jun/JNK activation and expression of MMPs by THP-M cells.

Inhibition of METTL3 prevents CS-induced emphysema in mice through blocking miR-93 regulation of the DUSP2/JNK signaling pathway

The effect of knockdown of METTL3 on CS-induced emphysema in the lung tissues of mice was evaluated. Adeno-associated virus (AAV) METTL3 shRNA or a

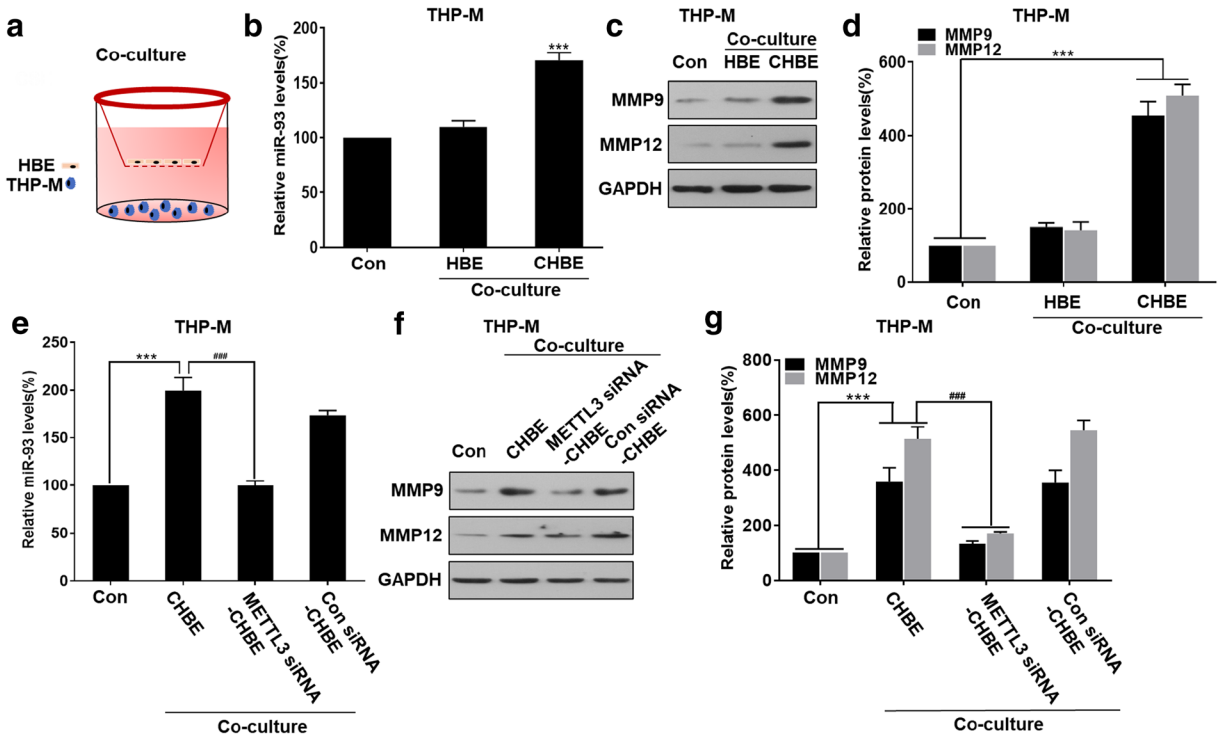

Fig. 3 Decreases of METTL3 in CHBE cells block the increases of miR-93 and MMPs levels in THP-M cells co-cultured with CHBE cells. Abbreviations: HBE, normal HBE cells; CHBE, HBE cells treated with CSE; METTL3-CHBE, HBE cells transfected with a METTL3 siRNA and then treated with CSE; Con siRNA-CHBE, HBE cells transfected with a control siRNA-CHBE and then treated with CSE. Densities of bands were quantified by the ImageJ software. GAPDH levels, measured in parallel, served as controls. After HBE cells were treated with 0 or 4% CSE for 48 h, THP-M cells were co-cultured with HBE cells or CHBE cells for 48 h. **a** Schematic representation of THP-M cells co-cultured with HBE cells or CHBE cells. **b** The levels of miR-93 in THP-M cells were determined by qRT-PCR. **c** Western blots were performed, and **d** relative protein levels of MM9 and MMP12 in THP-M cells were determined. THP-M cells were co-cultured with CHBE cells transfected with 20 nM of METTL3 siRNA or Con siRNA for 48 h. **e** The levels of miR-93 in THP-M cells were determined by qRT-PCR. **f** Western blots were performed, and **g** relative protein levels of MMP9 and MMP12 in THP-M cells were determined. Bars are presented as means ± SD ($n = 3$). $^{*}P < 0.05$, $^{**}P < 0.01$, and $^{***}P < 0.001$, different from control THP-M cells. $^{\#}P < 0.05$, $^{\#\#}P < 0.01$, and $^{\#\#\#}P < 0.001$, different from THP-M cells co-cultured with CHBE cells in the absence of METTL3 siRNA

negative control was injected via the nose at the fourth week of CS exposure. At 16 weeks later, mice were killed, and lung tissues were assayed (Fig. 8a). Lungs of mice receiving METTL3 shRNA had lower METTL3 levels, demonstrating that METTL3 was downregulated (Fig. 8e, f). H&E staining showed that, for CS-exposed mice, knockdown of METTL3 blocked changes in expanded airspaces (Fig. 8b, c). Further, CS-exposed mice treated with AAV METTL3 shRNA revealing lower expression of miR-93 (Fig. 8d). Moreover, the expressions of DUSP2 and elastin were restored for mice treated with METTL3 shRNA, whereas JNK pathway activation and MMP9 and MMP12 levels were decreased (Fig. 8e, f). Thus, METTL3 shRNA reverses the CS-induced effects associated with emphysema in mice, which are related to blocking miR-93 regulation of the DUSP2/JNK signaling pathway.

CS induces increases of EV miR-93 and the activation of the NK/c-Jun signaling pathway in human COPD

To elucidate the involvement of METTL3-mediated EV miR-93 in COPD pathogenesis, we isolated EVs from serum of non-smokers (n = 26), smokers (n = 25), and

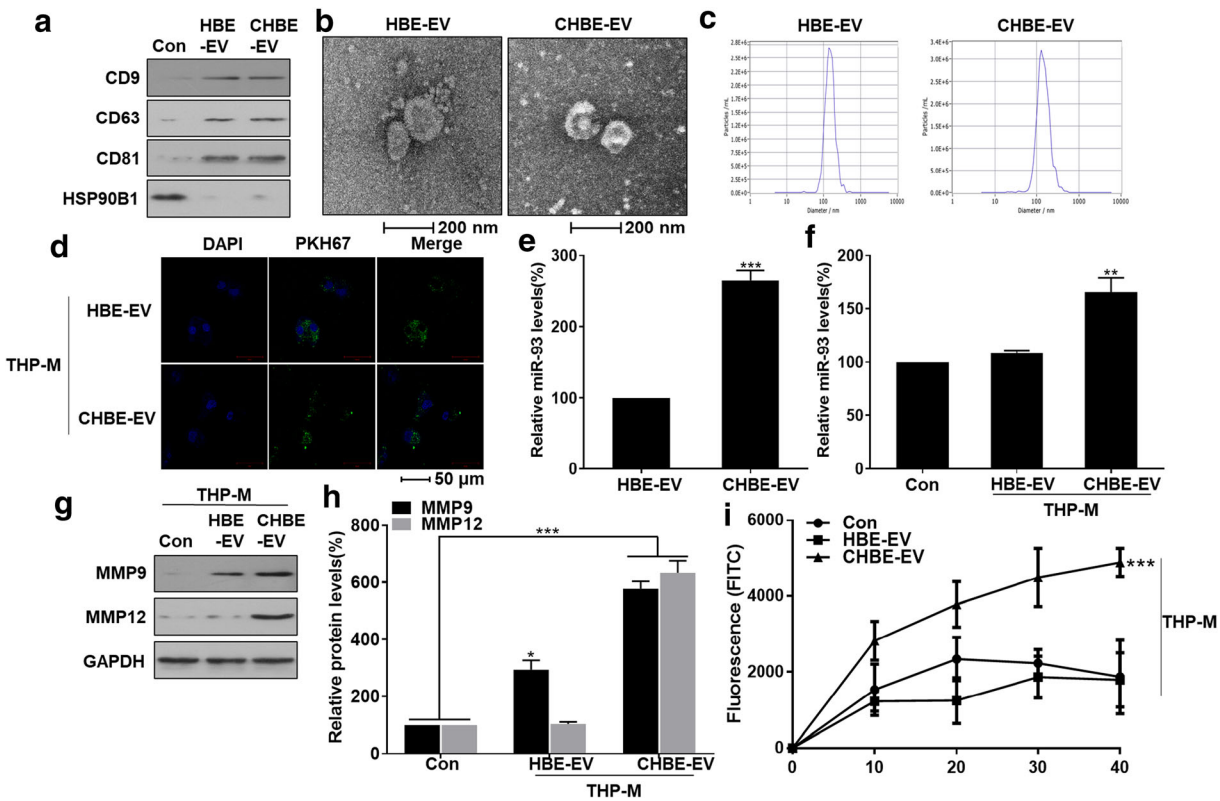

Fig. 4 EVs derived from CHBE cells transfer miR-93 to THP-M cells, which promotes the expression of MMPs in THP-M cells. Densities of bands were quantified by the ImageJ software. GAPDH levels, measured in parallel, served as controls. After HBE cells were treated with 0 or 4% CSE for 48 h, EVs from HBE and CHBE cells were fractionated by sequential ultracentrifugation as described previously. **a** Western blots of CD9, CD63, and CD81 in HBE-Exo or CHBE-Exo. **b** Electron microscopic images of HBE-EV and CHBE-EV (bars: 200 nm). **c** Particle number and size analysis of HBE-EV or CHBE-EV were determined by dynamic light scattering using a ZetaView® nanoparticle tracker (ParticleMetrix, Germany). **d** Microscopic images of THP-M cells after incubation with PKH67-labeled (green) HBE-EV or CHBE-EV; nuclei were stained with DAPI (blue) (bar: 50 μm). **e** The levels of miR-93 in HBE-EV or CHBE-EV were determined by qRT-PCR. $^{*}P < 0.05$, $^{**}P < 0.01$, and $^{***}P < 0.001$, different from HBE-EV. THP-M cells were treated with 50 μg/mL HBE-EV or CHBE-EV for 48 h. **f** The levels of miR-93 in THP-M cells were determined by qRT-PCR. **g** Western blots were performed, and **h** relative protein levels of MMP9 and MMP12 were determined in THP-M cells. **i** The production of fluorescein isothiocyanate (FITC) of THP-M cell culture medium was measured by BODIPY® FL-labeled elastin as described previously. Bars are presented as means ± SD (n = 3). $^{*}P < 0.05$, $^{**}P < 0.01$, and $^{***}P < 0.001$, different from control THP-M cells

COPD smokers (n = 26). Western blotting proved the existence of EVs markers (Fig. 9a). qRT-PCR revealed higher miR-93 levels in EVs from COPD smokers than in EVs from non-smokers and smokers (Fig. 9b). Furthermore, miR-93 levels negatively correlated with the percentages of FEV1/FVC in COPD patients (n = 26) (Fig. 9c). Moreover, expressions of DUPS2 and elastin in COPD lungs were lower than those in the

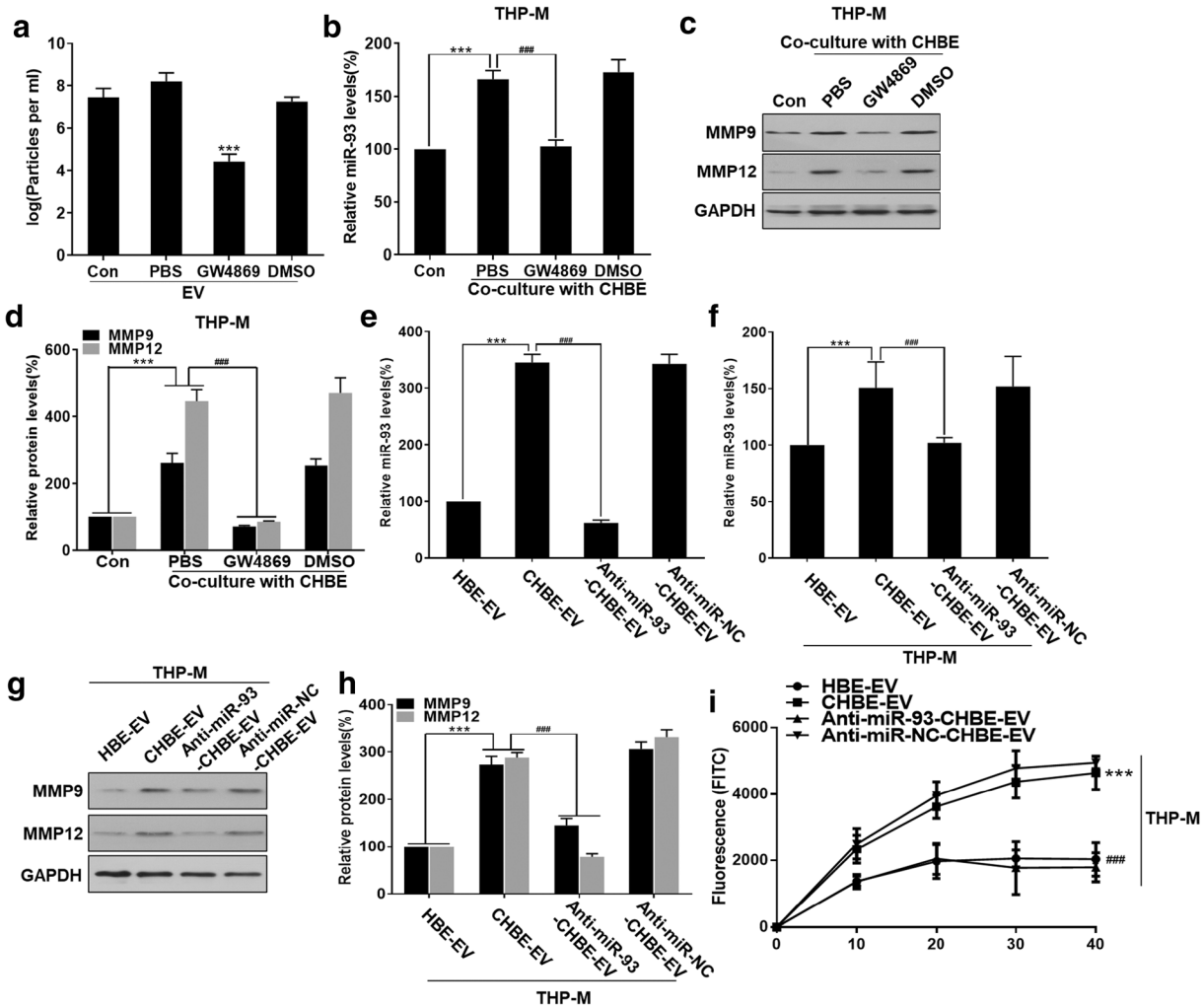

Fig. 5 EV miR-93 derived from CHBE cells promotes the expression of MMPs in THP-M cells. Densities of bands were quantified by the ImageJ software. GAPDH levels, measured in parallel, served as controls. After CHBE cells were treated with DMSO or GW4869 (an inhibitor of EVs generation) for 12 h, they were co-cultured with THP-M cells for 48 h. **a** Tracking analysis of nanoparticles from CHBE cells was accomplished for EVs isolated by sequential ultracentrifugation. **b** The levels of miR-93 in THP-M cells were determined by qRT-PCR. **c** Western blots were performed, and **d** protein levels of MMP9 and MMP12 in THP-M cells were determined. $^{*}P < 0.05$, $^{**}P < 0.01$, and $^{***}P < 0.001$, different from control THP-M cells. $^{\#}P < 0.05$, $^{\#\#}P < 0.01$, and $^{\#\#\#}P < 0.001$, different from THP-M cells co-cultured with CHBE cells treated with DMSO. After HBE cells were transfected with 50 nM of miR-93 inhibitor or Con inhibitor for 6 h, HBE cells were treated with 0 or 4% CSE for 48 h. **e** The levels of EV miR-93 derived from CHBE cells and HBE cells were determined by qRT-PCR. THP-M cells were treated with HBE-EV, CHBE-EV, anti-miR-93-CHBE-EV, or anti-miR-NC-CHBE-EV for 48 h. **f** The levels of miR-93 in THP-M cells were determined by qRT-PCR. **g** Western blots were performed, and **h** protein levels of MMP9 and MMP12 were determined. **i** The production of FITC of THP-M cell culture medium was measured by BODIPY® FL-labeled elastin as described previously. BODIPY® FL-labeled elastin as described previously. Bars are presented as means ± SD (n = 3). $^{*}P < 0.05$, $^{**}P < 0.01$, and $^{***}P < 0.001$, different from THP-M cells treated with HBE-EV. $^{\#}P < 0.05$, $^{\#\#}P < 0.01$, and $^{\#\#\#}P < 0.001$, different from THP-M cells treated with CHBE-EV in the absence of miR-93 inhibitor

lungs of smokers and COPD patients, whereas JNK pathway activation and MMP9 and MMP12 levels were increased (Fig. 9d, e). These results indicate that METTL3-mediated aberrant EV miR-93 is linked to activation of the JNK/MMPs axis in response to CS, resulting in induction of elastin degradation.

Discussion

CS, an important source of air pollutants in indoor environments, contains more than 6000 identified chemical constituents, some of which have strong oxidizing, pro-inflammatory, and carcinogenic properties (Rawlinson et al. 2017). Meanwhile, epidemiological evidence confirms that cigarette smoking is an risk factor of COPD (Hou et al. 2018). A causative role for MMPs is involved in the pathogenesis of CS-induced COPD and its serious sequelae, emphysema (Gharib et al. 2018). Excessive protease activity is associated with the pathophysiology of COPD (Nyunoya et al. 2014). Macrophages are thought to produce essentially all of these proteinases, which are associated with degradation of elastin in the walls of alveoli, resulting in the functional destruction of lung tissue (Lee et al. 2014). As the first-line of defense against inhaled environmental particles, the injured airway epithelium secretes inflammatory mediators to activate immune cell, such as macrophages (Moon et al. 2014). The present work reveals a mechanism for EVs-mediated intercellular cross-talk of epithelium–macrophages that implicated in the development and progression of CS-induced emphysema.

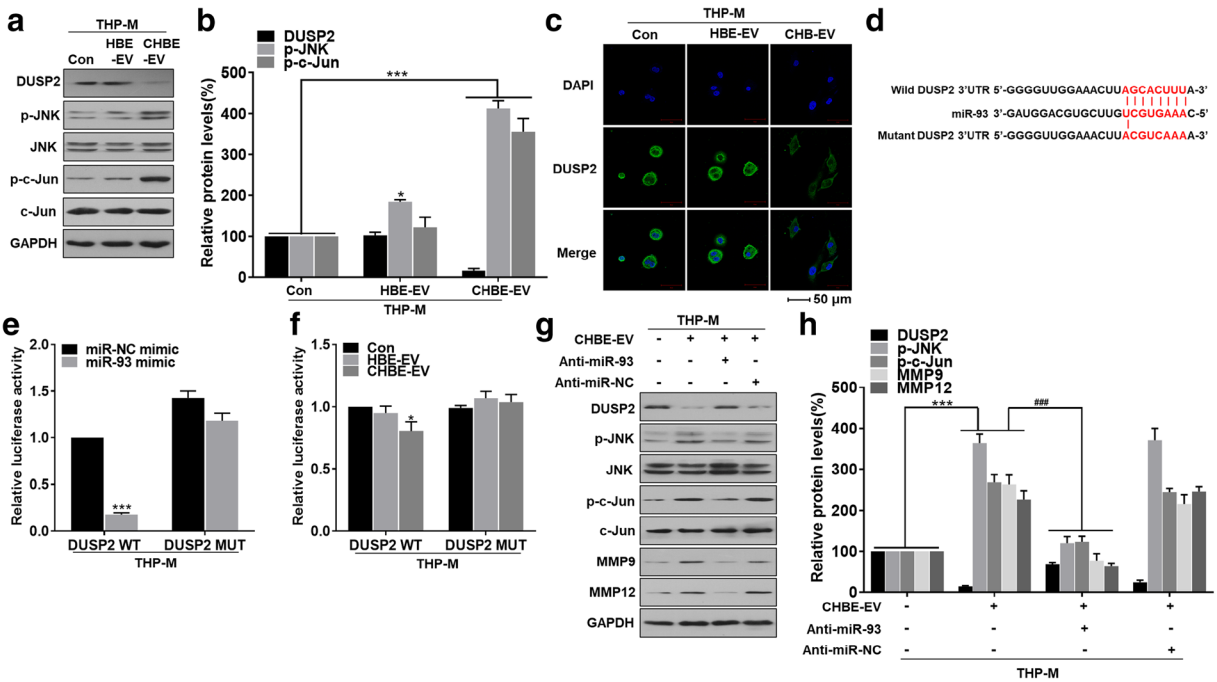

Fig. 6 EV miR-93 regulates JNK/c-Jun pathway activation by targeting DUSP2, which is involved in expression of MMPs in THP-M cells. THP-M cells were treated with 50 μg/mL HBE-EV or CHBE-EV for 48 h. **a** Western blots were performed, and **b** protein levels of DUSP2, p-JNK, and p-c-Jun in THP-M cells were determined. **c** Immunofluorescence staining of DUSP2 (green) in THP-M cells. Nuclei were stained with DAPI (blue) (bar: 50 μm). **d** Schematic of miR-93 putative target sites in the 3'UTR of DUSP2 and the sequences of mutant UTRs. THP-M cells co-transfected with 100 nM of miR-93 mimic or miR-NC mimic and 1 μg of DUSP2-wt plasmid or DUSP2-mut plasmid. **e** Luciferase reporter assays were performed on THP-M cells. **f** Luciferase readout from wild-type or mutant DUSP2 3′UTR reporter transfected into THP-M cells, which were then incubated with EVs (50 μg/mL) derived from normal or CHBE cells. THP-M cells were transfected with 50 nM of miR-93 inhibitor or miR-NC inhibitor and then incubated with 50 μg/mL CHBE-EV. **g** Western blots were performed, and **h** protein levels of DUSP2, p-JNK, p-c-Jun, MMP9, and MMp12 in THP-M cells were determined. All bars are presented as means ± SD ($n = 3$). $^{*}P < 0.05$, $^{**}P < 0.01$, and $^{***}P < 0.001$, different from control THP-M cells. $^{\#}P < 0.05$, $^{\#\#}P < 0.01$, and $^{\#\#\#}P < 0.001$, different from THP-M cells treated with CHBE-EV in the absence of miR-93 inhibitor

Emphysema has a complicated pathogenesis, related to various types of cellular dysfunction; destruction of the alveolar ECM is thought to be a causative event (Heinz 2020). MMPs, in particular those produced by macrophages, are involved in the pathogenesis of emphysema (Lee et al. 2014). MMP9 and MMP12 are involved in the degradation of alveolar ECM, specifically elastin, a causative event in development of emphysema (Shibata et al. 2018). In mice, overexpression MMP-9 in macrophages results in spontaneous emphysema (Foronjy et al. 2008). Further, *Mmp12*−/− mice are resistant to CS-related emphysema (Hautamaki et al. 1997; Houghton et al. 2009). These observations are in agreement with our findings that, with smoking, the levels of MMP-9 and MMP12 were increased in the lungs, but elastin levels were decreased. These changes were more pronounced in the lungs of smokers with emphysema. These findings indicate a role of MMP-9 and MMP12 in the development and progression of emphysema related to CS exposure.

CS is the main risk factor for COPD, and COPD patients who smoke have worse lung function; however, the mechanisms of the effects of CS remain to be established (Agusti and Hogg 2019). Epigenetic changes contribute to smoking-related COPD (Morrow et al. 2018). miRNAs, which regulate the expression of proteins related to oxidative stress and inflammatory responses, are involved in the development of emphysema (Rosas-Alonso et al. 2019). In the present study, we demonstrated that CSE elevated METTL3 expression in bronchial epithelial cells. The overexpression of METTL3 promoted miR-93 maturation via enhanced m6A modifications of pri-miR-93. In addition, miR-93 was elevated in the EVs of COPD smoker, and there was a negative correlation between miR-93 levels and FEV1/FVC. These results indicate that EV miR-93 serves as a biomarker for risk assessment of COPD.

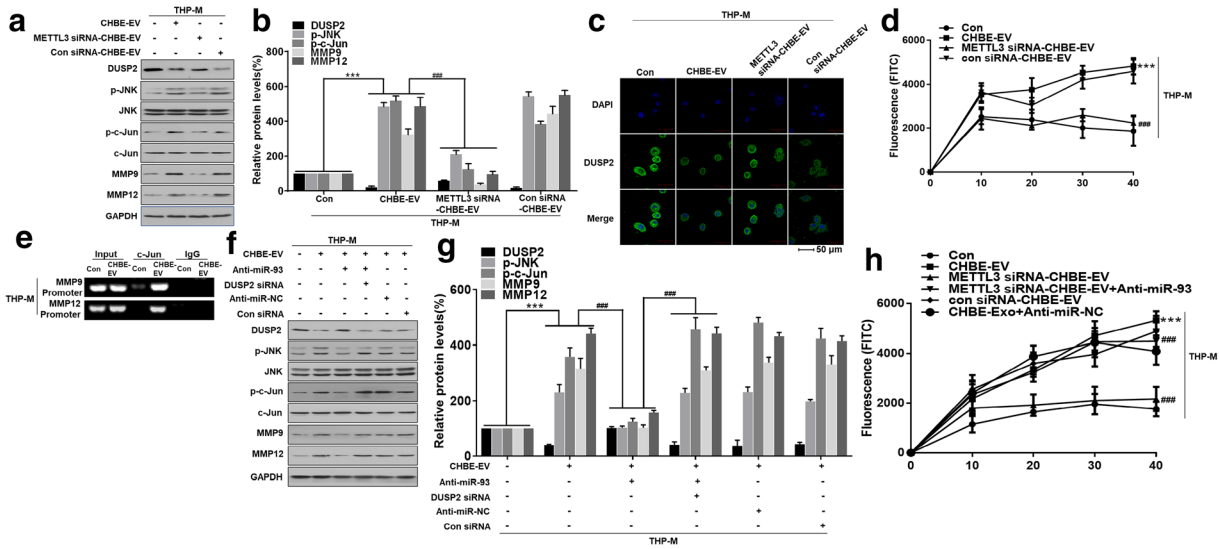

Fig. 7 METTL3-mediated EV miR-93, via DUSP2, is involved in JNK/c-Jun activation and expression of MMPs in THP-M cells. Densities of bands were quantified by the ImageJ software. GAPDH levels, measured in parallel, served as controls. THP-M cells were treated with 50 μg/mL CHBE-EV, METTL3 siRNA-CHBE-EV, or Con siRNA-CHBE-EV for 48 h. **a** Western blots were performed, and **b** relative protein levels of METTL3, DUSP2, p-JNK, p-c-Jun, MMP9, and MMP12 in THP-M cells were determined. **c** Immunofluorescence staining of DUSP2 (green) and nuclei stained with DAPI (blue) in THP-M cells (bar: 50 μm). **d** The FITC of THP-M cell culture medium was measured by BODIPY® FL-labeled elastin as described previously. $^{*}P < 0.05$ different from control THP-M cells. $^{\#}P < 0.05$ different from THP-M cells treated CHBE-EV. THP-M cells were transfected with 50 nM of miR-93 inhibitor or co-transfected with 20 nM of DUSP2 siRNA and then incubated with EVs (50 μg/mL) derived from CHBE cells. **e** The levels of MMP9 and MMP12 were measured by RT-PCR after the chromatin was immunoprecipitated with c-Jun Ab by ChIP assay. **f** Western blots were performed, and **g** relative protein levels of METTL3, DUSP2, p-JNK, p-c-Jun, MMP9, and MMP12 in THP-M cells were determined. **h** The FITC of THP-M cell culture medium was measured by BODIPY® FL-labeled elastin as described previously. All bars are presented as means ± SD ($n = 3$). $^{*}P < 0.05$, $^{**}P < 0.01$, and $^{***}P < 0.001$, different from control THP-M cells. $^{\#}P < 0.05$, $^{\#\#}P < 0.01$, and $^{\#\#\#}P < 0.001$, different from THP-M cells treated with CHBE-EV and anti-miR-93

JNK pathway mediates eukaryotic cell responses to a wide range of abiotic and biotic stresses (Zeke et al. 2016). In immune cells, DUSP2 and related proteins, which regulate JNK activity through dephosphorylation, are negative regulators (Jeffrey et al. 2006). The JNK pathway is activated in lipopolysaccharide-injured lungs (Schuh and Pahl 2009). In addition, MMPs, which are associated with lung injury, are regulated by the JNK pathway as well as by signal transducers (Son and Lee 2019). Our results showed that EV miR-93 triggers the JNK pathway via suppressing DUSP2. Phosphorylated c-Jun bound to the promoter of the MMP9 and MMP12 gene, facilitating its transcription. Furthermore, along with activation of the JNK pathway, there was elevation of MMP9 and MMP12 in the lungs of COPD patients.

The m6A modification in RNAs is a epigenetic change implicated in maturation of miRNAs (Gregory et al. 2004). m6A modifications label pri-miRNAs and recruit DGCR8 by METTL3-mediated m6A, thus promoting the maturation of miRNAs (Ma et al. 2017). Based on the present observations, overexpression METTL3 enhances the miR-93 levels in epithelial cells, and overproduced miR-93 is transported to macrophages via EVs, thus accelerating elastin degradation via activation of the JNK/MMPs axis, which leads to emphysema. Thus, we have demonstrated a role for METTL3 in CS-induced emphysema. Consistent with the results of in vitro experiments, METTL3 was overexpressed in the lungs of mice exposed to CS, and, for these mice, miR-93 upregulation and an JNK pathway activation. In mice, downregulation of METTL3 alleviated CS-induced elastin degradation and emphysema. Since m6A modifications are also present in other primary miRNAs, clarification of how these modifications affect processing of other miRNAs

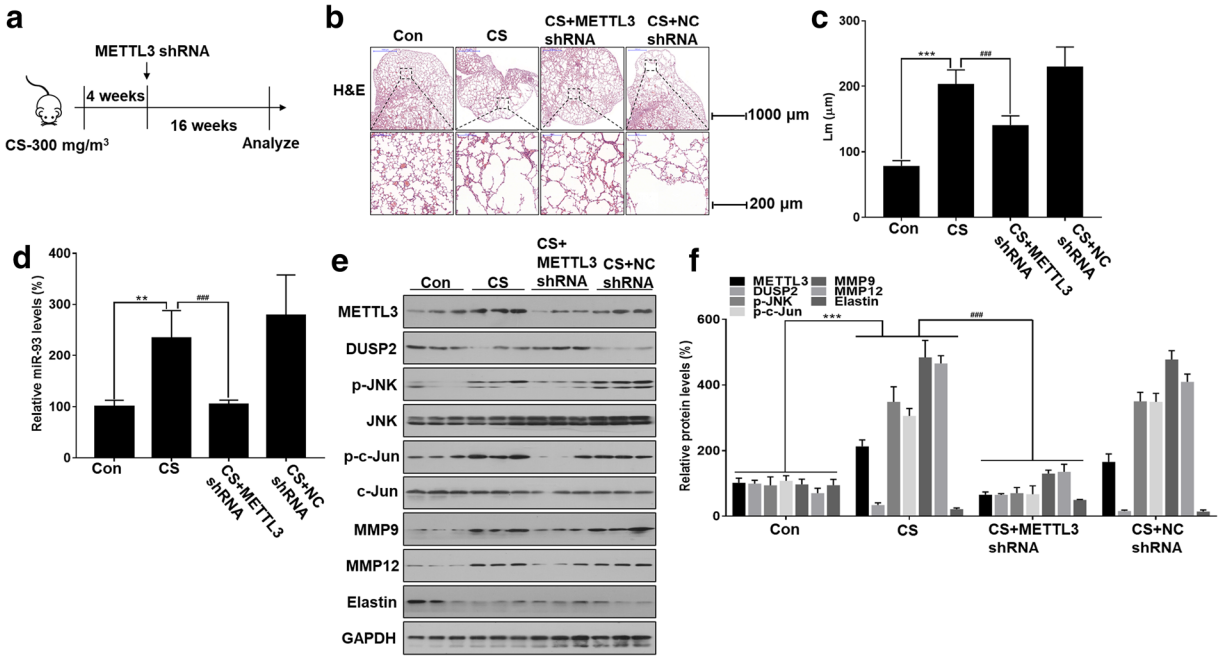

Fig. 8 Inhibition of METTL3 prevents CS-induced emphysema, the increases of METTL3 and miR-93 levels, the activation of DUSP2/JNK/c-Jun in lung tissues of mice. Densities of bands were quantified by the ImageJ software. GAPDH levels, measured in parallel, served as controls. Male BALB/c mice (age 6–8 weeks) were divided into four groups: normal control, CS, CS plus METTL3 shRNA, and CS plus NC shRNA. METTL3 shRNA and an shRNA negative control were administered by nose instillations. The mice were exposed to air or to CS (300 mg/m^3 TPM) every 5 days/week for 16 weeks. **a** A schematic diagram illustrating the experimental design. **b** Representative images of lung sections stained by H&E (bars: top = 1000 μm, bottom = 200 μm). **c** Quantification of mean chord length (Lm) in lung tissues of mice. **d** The levels of miR-93 in lung tissues of mice were determined by qRT-PCR. **e** Western blots were performed, and **f** relative protein levels of METTL3, DUSP2, p-JNK, p-c-Jun, MMP9, MMP12, and elastin in lung tissues of mice were determined. Bars are presented as means ± SEM ($n = 6$). $^{*}P < 0.05$, $^{**}P < 0.01$, and $^{***}P < 0.001$, different from control mice, $^{\#}P < 0.05$, $^{\#\#}P < 0.01$, and $^{\#\#\#}P < 0.001$, different from CS-exposed mice in the absence of METTL3 shRNA

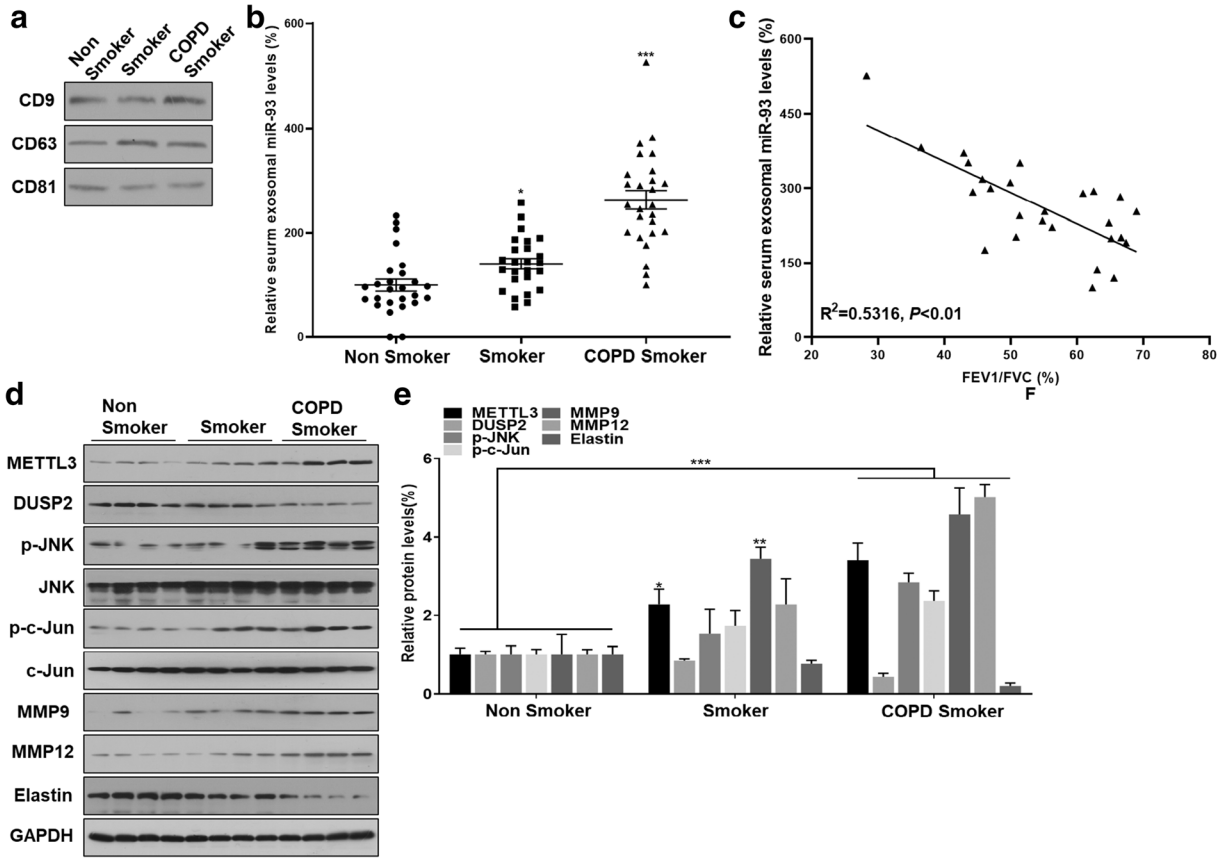

Fig. 9 CS induces increases of EV miR-93 in serum and the activation of JNK/c-Jun in lung tissues of people. EVs from serum of non-smokers ($n = 26$), smokers ($n = 25$), or COPD smokers ($n = 26$) were isolated. Densities of bands were quantified by the ImageJ software. GAPDH levels, measured in parallel, served as controls. **a** Western blots of CD9, CD63, and CD81 in serum EVs. **b** The levels of EV miR-93 in serum were determined by qRT-PCR. **c** The relationship between the levels of EV miR-93 in serum and FEV_1/FVC (%) in COPD smokers ($n = 26$). **d** Western blots were performed, and **e** relative protein levels of METTL3, DUSP2, p-JNK, p-c-Jun, MMP9, MMP12, and elastin in lung tissues of people ($n = 4$) were determined. Bars are presented as means ± SEM. $^*P < 0.05$, $^{**}P < 0.01$, and $^{***}P < 0.001$, different from normal lung tissue

would expand our knowledge about the development of emphysema.

EV miR-93, secreted from injured epithelial cells and taken up by macrophages, activated the JNK/MMPs axis via downregulation of DUSP2. DUSP2 expression, which is restricted to immune cells, was initially identified as a negative regulator of JNK signaling in macrophages (Jeffrey et al. 2006). We have provided evidence that miR-93 activates the JNK/MMPs axis via downregulation DUSP2, and we confirmed that DUSP2 downregulation and activated JNK signaling were evident in the lungs of COPD patients. In diabetic retinopathy, glucocorticoids attenuate IL-1β-induced galectin-1/LGALS1 via DUSP1 (Hirose et al. 2019). It would be interesting to examine the possible link between the glucocorticoid inducibility of DUSP2 and the lack of steroid sensitivity in smoking-related COPD.

In conclusion, for bronchial epithelial cells, CS exposure induces elevation of METTL3-promoted miR-93 maturation, and miR-93 is transferred from bronchial epithelial cells into macrophages by EVs. In macrophages, miR-93 activates the JNK pathway by targeting DUSP2, which increases the levels of MMP9 and MMP12, inducing elastin degradation. Therefore, CS induces emphysema by a mechanism in which METTL3-mediated EV miR-93 via m6A is involved in aberrant cross-talk of lung epithelial cells and macrophages. Our results show that aberrant m6A is involved in the pathogenesis of smoking-related emphysema.

Supplementary Information The online version contains supplementary material available at https://doi.org/10.1007/s10565-021-09585-1.

Acknowledgements The authors thank Donald L. Hill (University of Alabama at Birmingham, USA), an experienced, English-speaking scientific editor, for editing.

Author Contribution Haibo Xia and Yan Wu designed and wrote the manuscript; Haibo Xia, Yan Wu, and Jing Zhao performed in vivo experiments; Haibo Xia and Jing Zhao performed in vitro experiments; Wenqi li, Lu Lu and Huimin Ma analyzed the data; Tao Bian and Qizhan Liu assisted with the manuscript revision; and Quanyong Xiang and Qizhan Liu supervised the study.

Funding This work was supported by the Natural Science Foundations of China (81973085, 81803276, 81973005), the Top Talent Support Program for young and middle-aged people of Wuxi Health Committee (BJ2020006), and the Priority Academic Program Development of Jiangsu Higher Education Institutions (2019).

Materials availability All the data and materials presented in the current study along with additional files are available from the corresponding author on reasonable request.

Code availability Not applicable.

Declarations

Ethics approval All human samples procedures were approved by the Ethics Committee of Wuxi People's Hospital affiliated with Nanjing Medical University. All animal procedures were reviewed and approved by the Institutional Animal Care and Use Committee at Nanjing Medical University.

Consent for publication Not applicable.

Conflict of interest The authors declare no competing interests.

References

Agusti A, Hogg JC. Update on the pathogenesis of chronic obstructive pulmonary disease. N Engl J Med. 2019;381(13):1248–56. https://doi.org/10.1056/NEJMra1900475.

Alarcon CR, Lee H, Goodarzi H, Halberg N, Tavazoie SF. N6-methyladenosine marks primary microRNAs for processing. Nature. 2015;519(7544):482–5. https://doi.org/10.1038/nature14281.

Brinckerhoff CE, Matrisian LM. Matrix metalloproteinases: a tail of a frog that became a prince. Nat Rev Mol Cell Biol. 2002;3(3):207–14. https://doi.org/10.1038/nrm763.

Cheng M, Sheng L, Gao Q, Xiong Q, Zhang H, Wu M, et al. The m(6)A methyltransferase METTL3 promotes bladder cancer progression via AFF4/NF-kappaB/MYC signaling network. Oncogene. 2019;38(19):3667–80. https://doi.org/10.1038/s41388-019-0683-z.

Dang X, Qu X, Wang W, Liao C, Li Y, Zhang X, et al. Bioinformatic analysis of microRNA and mRNA regulation in peripheral blood mononuclear cells of patients with chronic obstructive pulmonary disease. Respir Res. 2017;18(1):4. https://doi.org/10.1186/s12931-016-0486-5.

De Smet EG, Van Eeckhoutte HP, Avila Cobos F, Blomme E, Verhamme FM, Provoost S, et al. The role of miR-155 in cigarette smoke-induced pulmonary inflammation and COPD. Mucosal Immunol. 2019;13:423–36. https://doi.org/10.1038/s41385-019-0241-6.

Elkington PT, Friedland JS. Matrix metalloproteinases in destructive pulmonary pathology. Thorax. 2006;61(3):259–66. https://doi.org/10.1136/thx.2005.051979.

Foronjy R, Nkyimbeng T, Wallace A, Thankachen J, Okada Y, Lemaitre V, et al. Transgenic expression of matrix metalloproteinase-9 causes adult-onset emphysema in mice associated with the loss of alveolar elastin. Am J Physiol Lung Cell Mol Physiol. 2008;294(6):L1149–57. https://doi.org/10.1152/ajplung.00481.2007.

Gharib SA, Manicone AM, Parks WC. Matrix metalloproteinases in emphysema. Matrix Biol. 2018;73:34–51. https://doi.org/10.1016/j.matbio.2018.01.018.

Gregory RI, Yan KP, Amuthan G, Chendrimada T, Doratotaj B, Cooch N, et al. The microprocessor complex mediates the genesis of microRNAs. Nature. 2004;432(7014):235–40. https://doi.org/10.1038/nature03120.

Gueders MM, Foidart JM, Noel A, Cataldo DD. Matrix metalloproteinases (MMPs) and tissue inhibitors of MMPs in the respiratory tract: potential implications in asthma and other lung diseases. Eur J Pharmacol. 2006;533(1-3):133–44. https://doi.org/10.1016/j.ejphar.2005.12.082.

Hautamaki RD, Kobayashi DK, Senior RM, Shapiro SD. Requirement for macrophage elastase for cigarette smoke-induced emphysema in mice. Science. 1997;277(5334):2002–4. https://doi.org/10.1126/science.277.5334.2002.

He S, Chen D, Hu M, Zhang L, Liu C, Traini D, et al. Bronchial epithelial cell extracellular vesicles ameliorate epithelial-mesenchymal transition in COPD pathogenesis by alleviating M2 macrophage polarization. Nanomed Nanotechnol Biol Med. 2019;18:259–71. https://doi.org/10.1016/j.nano.2019.03.010.

Heinz A. Elastases and elastokines: elastin degradation and its significance in health and disease. Crit Rev Biochem Mol Biol. 2020;55(3):252–73. https://doi.org/10.1080/10409238.2020.1768208.

Hirose I, Kanda A, Noda K, Ishida S. Glucocorticoid receptor inhibits Muller glial galectin-1 expression via DUSP1-dependent and -independent deactivation of AP-1 signalling. J Cell Mol Med. 2019;23(10):6785–96. https://doi.org/10.1111/jcmm.14559.

Hou HH, Wang HC, Cheng SL, Chen YF, Lu KZ, Yu CJ. MMP-12 activates protease-activated receptor-1, upregulates placenta growth factor, and leads to pulmonary emphysema. Am J Physiol Lung Cell Mol Physiol. 2018;315(3):L432–L42. https://doi.org/10.1152/ajplung.00216.2017.

Houghton AM, Hartzell WO, Robbins CS, Gomis-Ruth FX, Shapiro SD. Macrophage elastase kills bacteria within murine macrophages. Nature. 2009;460(7255):637–41. https://doi.org/10.1038/nature08181.

Janoff A, Raju L, Dearing R. Levels of elastase activity in bronchoalveolar lavage fluids of healthy smokers and nonsmokers. Am Rev Respir Dis. 1983;127(5):540–4. https://doi.org/10.1164/arrd.1983.127.5.540.

Jeffrey KL, Brummer T, Rolph MS, Liu SM, Callejas NA, Grumont RJ, et al. Positive regulation of immune cell function and inflammatory responses by phosphatase PAC-1. Nat Immunol. 2006;7(3):274–83. https://doi.org/10.1038/ni1310.

Jeon BN, Song JY, Huh JW, Yang WI, Hur MW. Derepression of matrix metalloproteinase gene transcription and an emphysema-like phenotype in transcription factor Zbtb7c knockout mouse lungs. FEBS Lett. 2019;593(18):2665–74. https://doi.org/10.1002/1873-3468.13501.

Lee JT, Pamir N, Liu NC, Kirk EA, Averill MM, Becker L, et al. Macrophage metalloelastase (MMP12) regulates adipose tissue expansion, insulin sensitivity, and expression of inducible nitric oxide synthase. Endocrinology. 2014;155(9):3409–20. https://doi.org/10.1210/en.2014-1037.

Lv Y, Liu W, Ruan Z, Xu Z, Fu L. Myosin IIA regulated tight junction in oxygen glucose-deprived brain endothelial cells via activation of TLR4/PI3K/Akt/JNK1/2/14-3-3epsilon/NF-kappaB/MMP9 signal transduction pathway. Cell Mol Neurobiol. 2019;39(2):301–19. https://doi.org/10.1007/s10571-019-00654-y.

Ma JZ, Yang F, Zhou CC, Liu F, Yuan JH, Wang F, et al. METTL14 suppresses the metastatic potential of hepatocellular carcinoma by modulating N(6)-methyladenosine-dependent primary MicroRNA processing. Hepatology. 2017;65(2):529–43. https://doi.org/10.1002/hep.28885.

Miao Q, Xu Y, Zhang H, Xu P, Ye J. Cigarette smoke induces ROS mediated autophagy impairment in human corneal epithelial cells. Environ Pollut. 2019;245:389–97. https://doi.org/10.1016/j.envpol.2018.11.028.

Moon HG, Kim SH, Gao J, Quan T, Qin Z, Osorio JC, et al. CCN1 secretion and cleavage regulate the lung epithelial cell functions after cigarette smoke. Am J Physiol Lung Cell Mol Physiol. 2014;307(4):L326–37. https://doi.org/10.1152/ajplung.00102.2014.

Morrow JD, Glass K, Cho MH, Hersh CP, Pinto-Plata V, Celli B, et al. Human lung DNA methylation quantitative trait loci colocalize with chronic obstructive pulmonary disease genome-wide association loci. Am J Respir Crit Care Med. 2018;197(10):1275–84. https://doi.org/10.1164/rccm.201707-1434OC.

Nyunoya T, Mebratu Y, Contreras A, Delgado M, Chand HS, Tesfaigzi Y. Molecular processes that drive cigarette smoke-induced epithelial cell fate of the lung. Am J Respir Cell Mol Biol. 2014;50(3):471–82. https://doi.org/10.1165/rcmb.2013-0348TR.

O'Farrell HE, Yang IA. Extracellular vesicles in chronic obstructive pulmonary disease (COPD). J Thorac Dis. 2019;11(Suppl 17):S2141–S54. https://doi.org/10.21037/jtd.2019.10.16.

Oglesby IK, McElvaney NG, Greene CM. MicroRNAs in inflammatory lung disease–master regulators or target practice? Respir Res. 2010;11:148. https://doi.org/10.1186/1465-9921-11-148.

Rawlinson C, Martin S, Frosina J, Wright C. Chemical characterisation of aerosols emitted by electronic cigarettes using thermal desorption-gas chromatography-time of flight mass spectrometry. J Chromatogr A. 2017;1497:144–54. https://doi.org/10.1016/j.chroma.2017.02.050.

Rosas-Alonso R, Galera R, Sanchez-Pascuala JJ, Casitas R, Burdiel M, Martinez-Ceron E, et al. Hypermethylation of anti-oncogenic microRNA 7 is increased in emphysema patients. Arch Bronconeumol. 2019;56:506–13. https://doi.org/10.1016/j.arbres.2019.10.017.

Schuh K, Pahl A. Inhibition of the MAP kinase ERK protects from lipopolysaccharide-induced lung injury. Biochem Pharmacol. 2009;77(12):1827–34. https://doi.org/10.1016/j.bcp.2009.03.012.

Seimetz M, Parajuli N, Pichl A, Veit F, Kwapiszewska G, Weisel FC, et al. Inducible NOS inhibition reverses tobacco-smoke-induced emphysema and pulmonary hypertension in mice. Cell. 2011;147(2):293–305. https://doi.org/10.1016/j.cell.2011.08.035.

Selman M, Cisneros-Lira J, Gaxiola M, Ramirez R, Kudlacz EM, Mitchell PG, et al. Matrix metalloproteinases inhibition attenuates tobacco smoke-induced emphysema in guinea pigs. Chest. 2003;123(5):1633–41. https://doi.org/10.1378/chest.123.5.1633.

Shibata S, Miyake K, Tateishi T, Yoshikawa S, Yamanishi Y, Miyazaki Y, et al. Basophils trigger emphysema development in a murine model of COPD through IL-4-mediated generation of MMP-12-producing macrophages. Proc Natl Acad Sci U S A. 2018;115(51):13057–62. https://doi.org/10.1073/pnas.1813927115.

Shipley JM, Wesselschmidt RL, Kobayashi DK, Ley TJ, Shapiro SD. Metalloelastase is required for macrophage-mediated proteolysis and matrix invasion in mice. Proc Natl Acad Sci U S A. 1996;93(9):3942–6. https://doi.org/10.1073/pnas.93.9.3942.

Sng JJ, Prazakova S, Thomas PS, Herbert C. MMP-8, MMP-9 and neutrophil elastase in peripheral blood and exhaled breath condensate in COPD. Copd. 2017;14(2):238–44. https://doi.org/10.1080/15412555.2016.1249790.

Son J, Lee SY. Ursonic acid exerts inhibitory effects on matrix metalloproteinases via ERK signaling pathway. Chem Biol Interact. 2019;315:108910. https://doi.org/10.1016/j.cbi.2019.108910.

Vogelmeier CF, Criner GJ, Martinez FJ, Anzueto A, Barnes PJ, Bourbeau J, et al. Global strategy for the diagnosis, management, and prevention of chronic obstructive lung disease 2017 report: GOLD Executive Summary. Eur Respir J. 2017;49(3). https://doi.org/10.1183/13993003.00214-2017.

Wahlgren J, De LKT, Brisslert M, Vaziri Sani F, Telemo E, Sunnerhagen P, et al. Plasma exosomes can deliver exogenous short interfering RNA to monocytes and lymphocytes. Nucleic Acids Res. 2012;40(17):e130. https://doi.org/10.1093/nar/gks463.

Wang J, Ishfaq M, Xu L, Xia C, Chen C, Li J. METTL3/m(6)A/miRNA-873-5p attenuated oxidative stress and apoptosis in colistin-induced kidney injury by modulating Keap1/Nrf2 pathway. Front Pharmacol. 2019;10:517. https://doi.org/10.3389/fphar.2019.00517.

Wu L, Tanimoto A, Murata Y, Fan J, Sasaguri Y, Watanabe T. Induction of human matrix metalloproteinase-12 gene transcriptional activity by GM-CSF requires the AP-1 binding site in human U937 monocytic cells. Biochem Biophys Res Commun. 2001;285(2):300–7. https://doi.org/10.1006/bbrc.2001.5161.

Xu H, Ling M, Xue J, Dai X, Sun Q, Chen C, et al. Exosomal microRNA-21 derived from bronchial epithelial cells is involved in aberrant epithelium-fibroblast cross-talk in COPD induced by cigarette smoking. Theranostics. 2018;8(19):5419–33. https://doi.org/10.7150/thno.27876.

Yang W, Bai J, Liu D, Wang S, Zhao N, Che R, et al. MiR-93-5p up-regulation is involved in non-small cell lung cancer cells proliferation and migration and poor prognosis. Gene. 2018;647:13–20. https://doi.org/10.1016/j.gene.2018.01.024.

Zeke A, Misheva M, Remenyi A, Bogoyevitch MA. JNK signaling: regulation and functions based on complex protein-protein partnerships. Microbiol Mol Biol Rev. 2016;80(3):793–835. https://doi.org/10.1128/MMBR.00043-14.

Zhang J, Bai R, Li M, Ye H, Wu C, Wang C, et al. Excessive miR-25-3p maturation via N(6)-methyladenosine stimulated by cigarette smoke promotes pancreatic cancer progression. Nat Commun. 2019;10(1):1858. https://doi.org/10.1038/s41467-019-09712-x.